Phys. Status Solidi A **208**, No. 6, 1364–1369 (2011) / **DOI** 10.1002/pssa.201001139

physica status solidi a
www.pss-a.com
applications and materials science

A silicon-based multi-sensor chip for monitoring of fermentation processes

M. Bäcker[1,2], S. Pouyeshman[1], Th. Schnitzler[1], A. Poghossian[1,2], P. Wagner[3], M. Biselli[1,2], and M. J. Schöning[*,1,2]

[1] Institute of Nano-and Biotechnologies, Aachen University of Applied Sciences, 52428 Jülich, Germany
[2] Peter Gruenberg Institute (PGI-8), Research Centre Jülich, 52425 Jülich, Germany
[3] Institute for Materials Research, Hasselt University, 3590 Diepenbeek, Belgium

Received 6 October 2010, revised 2 December 2010, accepted 22 December 2010
Published online 11 May 2011

Keywords electrochemical sensor, electrolyte conductivity, field-effect, process monitoring

[*] Corresponding author: e-mail schoening@fh-aachen.de, Phone: +49-241-600953215, Fax: +49-241-600953235

This paper describes the design and characterization of a silicon-based sensor chip for monitoring of fermentation processes. The sensor chip consists of three sensors using different transducer principles. A capacitive electrolyte-insulator-semiconductor (EIS) field-effect structure with Ta_2O_5 as gate material was utilized as pH sensor. An electrolyte conductivity sensor was realized by measuring the impedance between two interdigitated electrodes (IDE). A platinum thermistor was included for temperature measurements. The EIS sensor was integrated into a bioreactor and successfully used for an *inline* pH measurement. The layout of the IDE has been optimized with respect to a high cell constant and a wide detectable conductivity range. The integrated platinum thermistor allowed for temperature compensation of the electrolyte conductivity measurement.

1 Introduction The complex chemical structure of 'biopharmaceuticals' such as hormones, monoclonal antibodies or glycoproteins requires biotechnological processes for their synthesis. For this, microorganisms or mammalian cells that can be used as expression system have to be cultivated under optimal conditions since their metabolism strongly depends on external physical and chemical parameters [1, 2]. Deviations from ideal cultivation conditions may result in a reduced productivity as well as in changes of the expressed molecule, which can influence its therapeutic efficacy and physiological effect [3]. However, cellular systems are still poorly understood due to a lack of suited sensor systems matching the stringent conditions for bioprocess monitoring. In practice, temperature, pH value, dissolved oxygen concentration and the exhaust gas composition are the most widely measured and controlled *in situ* parameters [4, 5]. Even though vigorous research has been conducted, bioprocess optimization remains expensive and labor-intensive as manifold experiments have to be performed. Thus, miniaturization and parallelization for screening purposes whilst maintaining monitoring possibilities as on lab-scale reactors is of great interest [6]. Silicon-based electrochemical sensors are promising candidates to meet the stated requirements [7–10]. In this contribution, a silicon-based multi-sensor chip integrating different types of sensors is presented. The sensor chip comprises an electrolyte-insulator-semiconductor (EIS) field-effect structure for monitoring the pH value, a platinum thermistor for temperature measurements, and an impedance sensor based on interdigitated electrodes (IDE) for measuring the electrolyte conductivity. The chip represents one part of a sensor system that is developed as a tool for bioprocess monitoring [11].

2 Sensor working principles

2.1 Capacitive field-effect pH sensor Besides temperature, pressure and oxygen content, the pH value is the most frequently monitored parameter during a fermentation process as enzymatic activity and, thereby the complete metabolism is susceptible to pH variations [12]. In industrial fermentation plants and in lab-scale fermenters, pH monitoring by means of pH glass electrodes remains state-of-the-art [5]. However, as further miniaturization and parallelization of bioprocesses become more and more important, alternative monitoring devices are needed.

In this study, capacitive EIS structures with Ta_2O_5 as pH-sensitive transducer material have been used as pH

sensor. Owing to the simplicity in layout, the absence of a complicated encapsulation procedure and thus, an easier and cost-effective fabrication, non-glass capacitive EIS field-effect structures are well suited for (bio-)chemical sensor applications. Ta_2O_5 is well known for its outstanding properties for field-effect pH sensing, having a nearly Nernstian pH sensitivity as well as a high corrosion resistance in a wide pH range [13]. Additionally, the suitability of EIS structures for sterilization-in-place (SIP) and cleaning-in-place (CIP) has previously been demonstrated [11, 14].

2.2 Electrolyte conductivity sensor Planar IDE are commonly used electrode configurations for conductometric sensing applications [15, 16]. The cell geometry of each IDE has to be tailored depending on its purpose. An interdigitated comb-like structure can be defined by its amount of fingers, the finger length, the finger width and the finger spacing. Several theoretical considerations on optimizing the layout for measuring the electrolyte conductivity can be found in literature [17–20]. Two aspects are of predominant interest, (i) the cell constant of the conductivity sensor, and (ii) the frequency range for which its impedance response is solely resistive.

The relationship between the measured resistance R and the electrolyte conductivity κ is expressed by the cell constant K_{Cell}:

$$R = \frac{K_{\mathrm{Cell}}}{\kappa}. \tag{1}$$

Thus, for measurements in high ionic-strength solutions, like cell-culture medium, the cell constant should be relatively high in order to raise the resistance towards appropriate ranges. This can be realized by minimizing the size of the conductivity cell, for instance, by reducing the amount of fingers or decreasing the finger length. However, this modification at the same time reduces the double-layer capacitance and thereby, increases the interface impedance. This leads to a narrow frequency range for which the measured impedance of the system has a resistive nature.

Obtaining a wide frequency range is important for an application, as it allows the sensor to be run at a specific frequency, whilst covering a large conductivity range. The impedance response is frequency-dependent since the response is a result of the interplay of capacitive and resistive influences. The capacitive influences are related to the charging and discharging of the electrical double-layer at the interface electrode/electrolyte as well as to direct capacitive coupling between the electrodes. The latter case is described by the cell capacitance C_{Cell} and is directly related to the cell constant:

$$C_{\mathrm{Cell}} = \frac{\varepsilon_{\mathrm{electrolyte}} \cdot \varepsilon_0}{K_{\mathrm{Cell}}}. \tag{2}$$

Both requirements can be met by choosing proper geometric dimensions. The optimal ratio between finger spacing and finger width to increase the resistive regime of the conductivity sensor was found to be of 0.54 [21].

2.3 Temperature sensor Since cell growth and production rate have a strain-dependent distinct temperature optimum, the temperature should be maintained during the process and thus needs to be monitored [5]. Furthermore, the measurement of electrolyte conductivity has to be compensated for influences of temperature and referred to a standard temperature to be comparable [22]. The resistance of metallic thin films is often used as a measure for the temperature, especially in miniaturized devices. With raising temperature, the movement of charge carriers in the metal is increasingly hindered. As a result, the resistance of the metallic layer increases. The relation between electrical resistance and temperature is nearly linear over a wide range for platinum. The temperature coefficient of resistance of platinum equals $3.85 \times 10^{-3}/^{\circ}\mathrm{C}$ for bulk material.

3 Experimental

3.1 Sensor design Each of the single sensors poses constraints to the design that have to be addressed. For the pH sensor, Ta_2O_5 was chosen as pH-sensitive transducer material. Therefore, one part of the sensor chip has to have Ta_2O_5 as top layer that is in direct contact with the electrolyte. The interdigitated structure was dimensioned based on the assumptions explained in Section 2.2. The developed structure consisted of five fingers having a finger width of 600 μm, a finger spacing of 324 μm and a finger length of 2900 μm. The theoretical cell constant of this structure was calculated as $1.38\,\mathrm{cm}^{-1}$. The temperature sensor was designed to have a theoretical resistance at room temperature of $R_{20} = 100\,\Omega$. Thus, the layout comprised a meander-shaped platinum strip having a thickness of 200 nm, a length of 9.5 mm and a width of 50 μm. The additional platinum electrode on the chip is intended to serve as conducting track for a future screen-printed Ag/AgCl reference electrode (see Fig. 1).

3.2 Processing of the sensor chip The sensor chip was fabricated on a p–Si–SiO_2 substrate (30 nm thermally grown SiO_2) using standard microfabrication techniques.

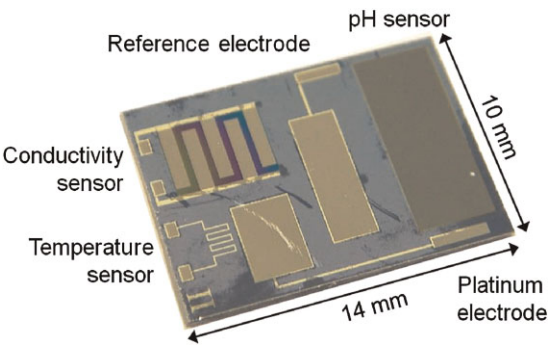

Figure 1 (online colour at: www.pss-a.com) Photograph of the developed sensor chip.

30 nm tantalum was deposited onto this substrate by means of electron-beam evaporation. Subsequent oxidation (517 °C, 30 min in oxygen atmosphere) of the tantalum resulted in a Ta_2O_5 layer having a thickness of about 60 nm, serving as pH-sensitive gate insulator material of the capacitive field-effect structure. A 300 nm Al film was then deposited as a rear-side contact layer for the field-effect sensor. Afterwards, the complete wafer was covered with successive layers of SiO_2, Si_3N_4 and SiO_2 (140, 500, 140 nm, respectively) deposited by means of plasma-enhanced chemical vapour technique to avoid influences from parasitic capacitances of the following electrode structures. These layers were then partly removed by reactive-ion etching (RIE) to uncover the Ta_2O_5 for the pH-sensitive region of the chip. All metallic structures consisted of 20 nm titanium as an adhesion layer and 200 nm platinum as electrode material. The metallic layers were formed by electron-beam evaporation and structured by conventional photolithographic processes. A second passivation layer consisting of SiO_2, Si_3N_4 and SiO_2 was deposited in order to passivate the conductive paths and subsequently etched to expose the sensitive sensor parts. Finally, the wafer was separated into chips, these were cleaned and glued onto PCB substrates. Electrical connection was provided by means of an ultrasonic wedge bonder.

3.3 Measurement setup The electrochemical characterization of the EIS sensor consisted of capacitance-voltage (*C–V*) and constant-capacitance (ConCap) measurements. In the ConCap mode the dynamic characteristics of the EIS sensors are investigated. A DC polarization voltage is applied via the reference electrode (conventional liquid-junction Ag/AgCl electrode) to set the working point of the EIS sensor, and a small AC voltage is superimposed to measure the capacitance. By using a feedback-control circuit the capacitance of the EIS structure is kept constant. Thus, potential changes at the Ta_2O_5/electrolyte interface are directly monitored. For more details of the principle, see *e.g.* [23]. The measurements were carried out at a frequency of 275 Hz. For characterization of the IDE, electrochemical impedance spectroscopy in various KCl solutions and cell-culture medium was applied. The measurements were performed using an impedance analyzer (Zahner Elektrik). A four-electrode conductivity sensor with integrated temperature sensor served as reference (Mettler Toledo, InLab 730 connected to Mettler Toledo SevenMulti™ conductivity meter). The temperature measurements were performed in a temperature-controlled water bath (Lauda Ecoline RE-207) with a Keithley SourceMeter 2400 in four-wire configuration.

4 Results and discussion

4.1 pH sensor results For the experiments, the sensor was integrated into a lab-scale fermenter, sealed by an O-ring and contacted on its front side by the electrolyte and on its rear side by a gold-plated pin (see Fig. 2). A commercial pH glass electrode was also installed into the fermenter for comparison. After sterilization by means of autoclaving, the pH value of the cell-culture medium was continuously monitored with both the commercial glass electrode and the EIS sensor. The recorded signal of the pH glass electrode and the ConCap response of the EIS sensor are depicted in Fig. 3. As a result to induced pH changes both sensors displayed similar signal behaviour. The deviations of the EIS sensor signal are attributed to air bubbles that accumulated at the sensor surface. The pH sensitivity as derived from Fig. 3 amounts to about 50 mV/pH, which is slightly lower than literature values for Ta_2O_5 [13].

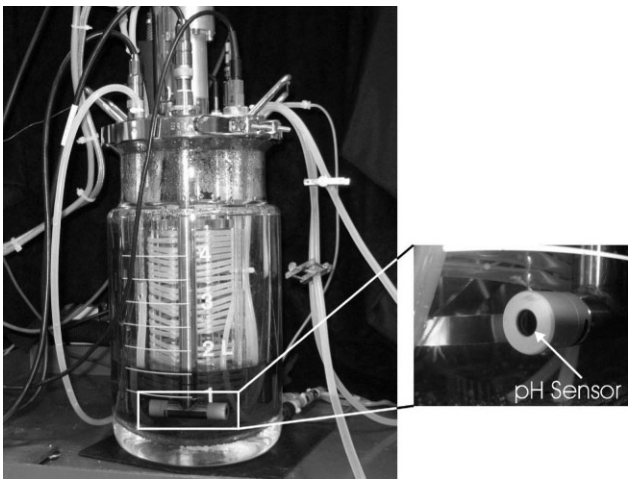

Figure 2 Integration of the EIS sensor into a bioreactor for *inline* measurements.

4.2 Conductivity sensor results The interdigitated structure has been characterized by electrochemical impedance spectroscopy in conductivity standard solutions having defined conductivities at 25 °C of 84 μS/cm, 1413 μS/cm and 12.88 mS/cm, respectively. The experimentally determined cell constant was found to be 1.29 cm^{-1} that is on good correlation to the theoretical value of

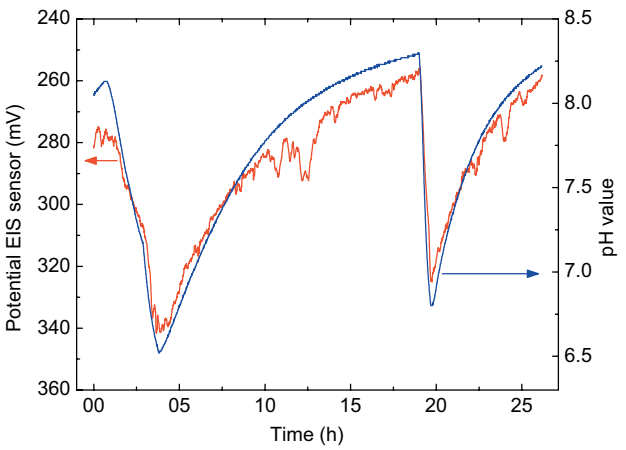

Figure 3 (online colour at: www.pss-a.com) *Inline* monitoring of the pH value – comparison between pH electrode and ConCap response of the EIS sensor.

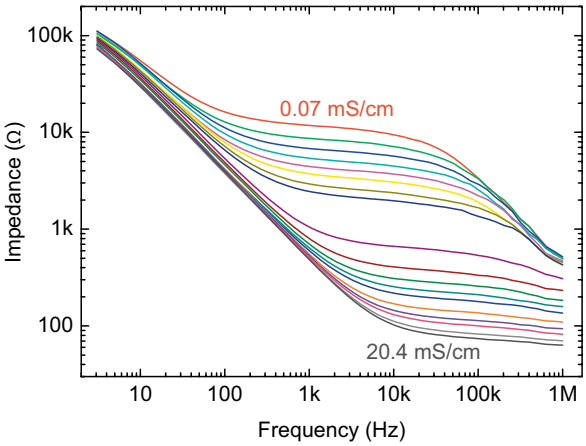

Figure 4 (online colour at: www.pss-a.com) Impedance spectra with the developed IDE in KCl solutions of different conductivities ranging from 0.07 to 20.4 mS/cm.

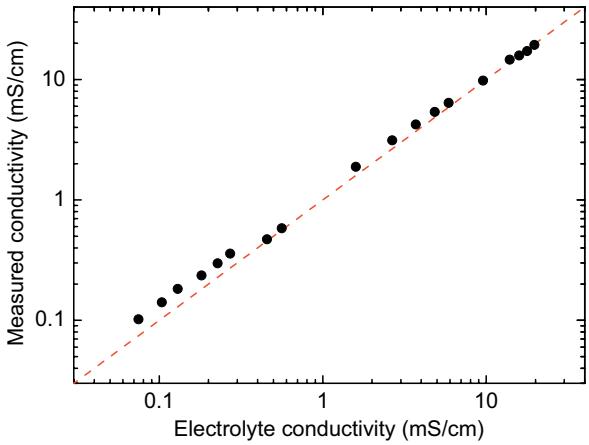

Figure 5 (online colour at: www.pss-a.com) Measured electrolyte conductivity with the developed IDE.

$1.38\,\mathrm{cm}^{-1}$. Figure 4 shows impedance spectra recorded with the conductivity sensor in KCl solutions of different conductivities ranging from 0.07 to 20.4 mS/cm. A clear dependence of the sensor response from the electrolyte conductivity was observed. The spectra can be divided into three regions, a low-frequency region, for which the impedance is dominated by the double-layer capacitance, a merely resistive impedance, where the response depends on the resistivity of the electrolyte and a high-frequency region, where capacitive behaviour was observed. With increasing electrolyte conductivity, the resistive impedance regime shifted to higher frequencies. For lower electrolyte conductivities, parallel capacitances dominate the impedance behaviour at frequencies above approximately 100 kHz, introducing a second cut-off frequency. This second cut-off frequency was not observed for higher electrolyte conductivities, since the electrolyte resistance remained the dominating part of the measured impedance in this high-frequency region.

Using the same measurement data, the electrolyte conductivity at distinct frequencies as measured by the IDE is plotted *versus* the conductivity as measured by the reference sensor (Fig. 5). The obtained conductivity values showed a good correlation to the values as measured by the reference sensor. Slightly higher values were measured in the conductivity range below 300 μS/cm.

Due to the optimized sensor design, the bandwidth between the two cut-off frequencies for which the response is strongly dependent on the electrolyte resistance was more than two decades wide. However, the complete conductivity range as tested could not be measured using only a single frequency.

4.3 Temperature sensor results The temperature sensor was characterized in a water bath in the range of 20–45 °C, revealing a temperature coefficient of $3.35 \times 10^{-3}/^{\circ}\mathrm{C}$. The resistance equaled $R_{20} = 100.9\,\Omega$. This is in close agreement with the intended value even though foil masks were used for the photolithography.

4.4 Combined conductivity and temperature measurement To investigate the possible compensation of temperature variations on the conductivity reading, additional measurements in the cell-culture medium were performed in a temperature-controlled water bath. The temperature and electrolyte conductivity were recorded with both, the chip sensor and the reference sensor and linear temperature compensation was performed according to Eq. (3).

$$\kappa_{\mathrm{Ref}} = \frac{\kappa}{1 + \frac{\alpha}{100\%}(T - T_{\mathrm{Ref}})}. \tag{3}$$

The reference temperature T_{Ref} was 25 °C. The linear temperature coefficient α of the cell-culture medium has been determined to be 2.03%/°C. The result of the simultaneous measurement of conductivity and temperature in the cell-culture medium is depicted in Fig. 6. During the first part of the experiment (0:00–1:45 h), the temperature was increased stepwise from 25–37 °C. Both sensors, chip-based and reference responded to the temperature change. However, the reference sensor displayed a decreased temperature value during the complete course of the experiment. As expected, the uncompensated conductivity measurement followed the increasing temperature. In contrast, by applying the linear temperature compensation the measured conductivity remained steady for both sensors.

During the second part of the experiment (1:45–2:40 h), the temperature was maintained at 37 °C and the conductivity of the cell-culture medium was altered by addition of KCl solution. Due to the increased ion concentration the electrolyte conductivity rose, too. The results for the uncompensated conductivity measurement demonstrated a good conformity between the chip sensor and the reference sensor. However, the temperature-compensated values of the chip sensor were systematically lower than those of the

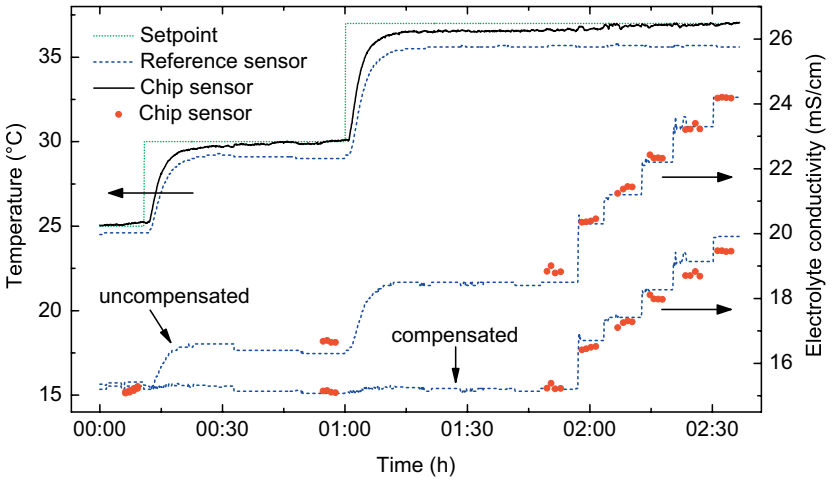

Figure 6 (online colour at: www.pss-a.com) Simultaneous recording of electrolyte conductivity (lower part of the graph) and temperature (upper part of the graph) with the sensor chip and comparison to reference sensor.

reference sensor. The reason for this is the difference of the two temperature sensors. As a result of the smaller temperature value as measured by the reference sensor, the denominator in Eq. (3) becomes lower, which leads to a higher compensated conductivity value.

5 Conclusions A silicon-based multi-sensor chip for monitoring of fermentation processes is presented. The chip integrates several sensors based on different transducer principles. A capacitive field-effect EIS structure with Ta_2O_5 as gate material was used as pH sensor. The sensor was integrated into a lab-scale bioreactor and was successfully used for pH monitoring for more than 1 day. The obtained pH sensitivity was about 50 mV/pH. The layout of IDE has been tailored for measuring the electrolyte conductivity in cell-culture medium. The main characteristics of the developed electrodes are a high cell constant of 1.29 cm^{-1} and a wide bandwidth of more than two decades for which the impedance response is merely resistive. Together with the integrated temperature sensor the conductivity sensor was successfully applied for performing temperature-compensated electrolyte conductivity measurements in cell-culture medium. Future works will be directed to the integration of a reference electrode [24] on the chip and *inline* measurements of temperature and conductivity during the fermentation process. In general, the set-up might be extended for addressing both physical and (bio-)chemical parameters by means of one single transducer platform [25], integrating a diffusion barrier when utilizing enzymatic sensor parts [26] or proofing alternative field-effect device concepts, like light-addressable potentiometric sensors [27, 28].

Acknowledgements The authors would like to thank the Federal Ministry of Education and Research (BMBF) for financial support within the frame of the project 'Cellsens'.

References

[1] M. Känsäkoski, M. Kurkinen, N. von Weymarn, P. Niemelä, P. Neubauer, E. Juuso, T. Eerikäinen, S. Turunen, S. Aho, and P. Suhonen, Process Analytical Technology (PAT) Needs and Applications in the Bioprocess Industry (VTT, Vuorimiehentie, Finland, 2006), p. 1.
[2] R. Ulber, B. Hitzmann, and T. Scheper, Chem. Ing. Tech. **73**, 19 (2001).
[3] P. Hossler, S. F. Khattak, and Z. J. Li, Glycobiology **19**, 936 (2009).
[4] F. Clementschitsch and K. Bayer, Microb. Cell Fact. **5**, 19 (2006).
[5] B. Sonnleitner, Adv. Biochem. Eng. Biotechnol. **66**, 1 (2000).
[6] M. A. Hanson, X. Ge, Y. Kostov, K. A. Brorson, A. R. Moreira, and G. Rao, Biotechnol. Bioeng. **97**, 833 (2007).
[7] E. E. Krommenhoek, J. G. E. Gardeniers, J. G. Bomer, X. Li, M. Ottens, G. W. K. van Dedem, M. van Leeuwen, W. M. van Gulik, L. A. M. van der Wielen, J. J. Heijnen, and A. van den Berg, Anal. Chem. **79**, 5567 (2007).
[8] T. Geisler, J. Ressler, H. Harz, B. Wolf, and R. Uhl, IEEE Trans. Autom. Sci. Eng. **3**, 169 (2006).
[9] M. Brischwein, E. R. Motrescu, E. Cabala, A. M. Otto, H. Grothe, and B. Wolf, Lab Chip. **3**, 234 (2003).
[10] M. J. Schöning and H. Lüth, Phys. Status Solidi A **185**, 65 (2001).
[11] M. Bäcker, S. Beging, M. Biselli, A. Poghossian, J. Wang, W. Zang, P. Wagner, and M. J. Schöning, Electrochim. Acta **54**, 6107 (2009).
[12] M. L. Shuler and F. Kargi, Bioprocess Engineering: Basic Concepts (Prentice Hall, Englewood Cliffs, NJ, 1992).
[13] A. Poghossian and M. J. Schöning, Silicon-based Chemical and Biological Field-effect Sensors: Encyclopedia of Sensors (American Scientific Publishers, Stevenson Ranch, USA, 2006), p. 463.
[14] M. J. Schöning, D. Brinkmann, D. Rolka, C. Demuth, and A. Poghossian, Sens. Actuators B **111/112**, 423 (2005).
[15] B. Hoffmann, M. Gadau, M. Paeschke, and R. Hintsche, Conductivity measurements with miniaturized thin film metal electrodes, in: The 8th International Conference on Solid-State Sensors and Actuators, 1995 and Eurosensors IX. Transducers '95, June 25–29, 1995), p. 837.
[16] N. F. Sheppard, R. C. Tucker, and C. Wu, Anal. Chem. **65**, 1199 (1993).
[17] B. Timmer, W. Sparreboom, W. Olthuis, P. Bergveld, and A. van den Berg, Lab Chip. **2**, 121 (2002).
[18] P. Jacobs, A. Varlan, and W. Sansen, Med. Biol. Eng. Comput. **33**, 802 (1995).

[19] V. F. Lvovich, C. C. Liu, and M. F. Smiechowski, Sens. Actuators B **119**, 490 (2006).
[20] D. He, M. A. Shannon, and N. R. Miller, IEEE Sens. J. **5**, 1185 (2005).
[21] G. R. Langereis, An integrated sensor system for monitoring washing processes, PhD thesis, Enschede (1999).
[22] Z. Moron, Considerations on the accuracy of measurements of electrical conductivity of liquids, in: XVIII IMEKO World Congress – Metrology for a Sustainable Development, September, 17–22, (2006).
[23] A. Poghossian, S. Ingebrandt, M. H. Abouzar, and M. J. Schöning, Appl. Phys. A: Mater. Sci. Process. **87**, 517 (2007).
[24] A. Simonis, H. Lüth, J. Wang, and M. J. Schöning, Sens. Actuators B **103**, 429 (2004).
[25] A. Poghossian and M. J. Schöning, Electroanalysis **16**, 1863 (2004).
[26] A. Poghossian, M. Thust, M. J. Schöning, M. Müller-Veggian, P. Kordos, and H. Lüth, Sens. Actuators B **68**, 260 (2000).
[27] T. Yoshinobu, H. Iwasaki, Y. Ui, K. Furuichi, Y. Ermolenko, Y. Mourzina, T. Wagner, N. Näther, and M. J. Schöning, Methods **37**, 94 (2005).
[28] T. Wagner, R. Molina, T. Yoshinobu, J. P. Kloock, M. Biselli, M. Canzoneri, T. Schnitzler, and M. J. Schöning, Electrochim. Acta **53**, 305 (2007).